

A COUPLED AERO AND STRUCTURAL DYNAMICS MODEL FOR COMPUTATION OF UNSTEADY LOADS ON THE HELICOPTER SKELDAR V200

Per Persson* and Per Weinerfelt*

Saab Aeronautics

SE-58188 Linköping

Keywords: Aerodynamics, Structure dynamics, unsteady loads

Abstract

The objective of this paper is to present a coupled aero and structural simulation model for the helicopter Skeldar V200. The complete simulation system consists of structural models for the helicopter frame, aero elastic models for the rotor blades, models for servos, swash plate and the control linkage between the swash plate and the rotor blades. Control laws simplifying the control and trimming of the helicopter are also included. The models are implemented in the Multi Body Dynamics (MBD) software MSC/Adams.

Comparisons between data from Adams simulations, rig tests and flight test data are presented in the present paper.

1. Introduction

Since 2005 Saab Aeronautics has been developing the unmanned autonomous helicopter Skeldar (initially in R&D program, later years in product development). The helicopter is designed for both military and commercial applications with VTOL and hovering capacity. The present paper focus on the present version of the helicopter V200 (see Fig 1). The outline of the paper is the following. The different simulation models are presented in section 2, the assembled model is discussed, in section 3. Section 4 presents results from investigations. Finally conclusions are given in Section 5.



Fig. 1 The autonomous helicopter Skeldar V200

2. Description of the simulation model

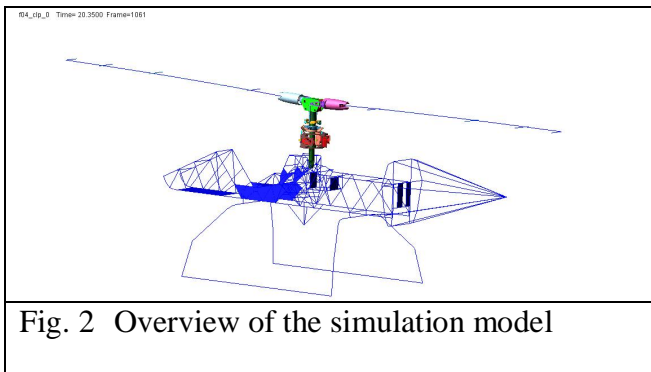
The numerical simulation model consists of three major parts outlined below. The structural dynamics, aerodynamics and control system parts are coupled to form a multi physics simulation model. The complete model is implemented in the commercial Multi Body Dynamics (MBD) system MSC/Adams.

2.1 Structural dynamics

The structural parts of the helicopter are defined in a CATIA CAD model and imported into Adams. Adams supports nonlinear and large structural motions, and with newer versions there are no serious reductions in accuracy or limitations in what terms are included in the description of motion. Gyroscopic forces, Coriolis effects and more traditional inertia forces are now fully included and confirmed in smaller test models. Apart from obvious

geometric representations from CAD, the structural dynamics model includes kinematic couplings between all moving parts. Mass and inertia for all parts are either calculated directly from CAD-data, or adjusted to represent also omitted smaller parts, e.g. bolts and plates etc. Most rotor system parts are rigid, but the frame and the blades are deformable, as well as some spring elements where applicable. The main helicopter frame is represented by a modal solution of a beam model, correlated to tests. However, in all analyses below, the helicopter frame is made rigid. The interaction between a flexible frame, flexible couplings and the rotor system is known to be difficult. If possible, care should be taken to avoid couplings that conflict with the rotor system dynamics. The current study is mainly focused on the rotor system, and in the current configuration the helicopter frame and coupling of the rotor system to the frame is of less concern.

An overview of the geometries in the simulation model is given in Fig. 2



2.2 The helicopter main rotor blades

The rotor blades obviously play a fundamental role in the dynamics in a rotor system. Therefore a somewhat more detailed description of the blade is necessary.

A few different models/designs of the rotor blades exist. Also different versions for the same blade model are implemented. A full 3D FE-model of the blades has been implemented and tested, but for efficiency reasons (primarily in post processing), the blades are better represented by a beam model. Both models

yield the same results as far as loads and dynamics are concerned. The blade models are correlated to physical tests and perform well within acceptable criteria.

The blades are included in the numerical model using a modal representation. As such, the numerical integration and use is fairly cheap and since there should be no material non-linearities involved in blade deformation, the modal approach should work fine. The MBD system takes care of the large rotation involved, and if small enough sub-models are used for the blade, the complete force situation is represented with good accuracy. For the time being, the current rotor blades are divided into 8 smaller segments to get better centrifugal loads allowing for linear treatment of the deformation within each segment, and non-linear effects are handled by the shifting/rotation of the sub system local coordinate systems. Each segment contains about 25 beam elements with varying beam characteristics. Blade modes up to several hundred Hertz are included, but main load and motion contributions come from the first few lower modes.

Blade characteristics in a rotating setup are given in Fig. 3

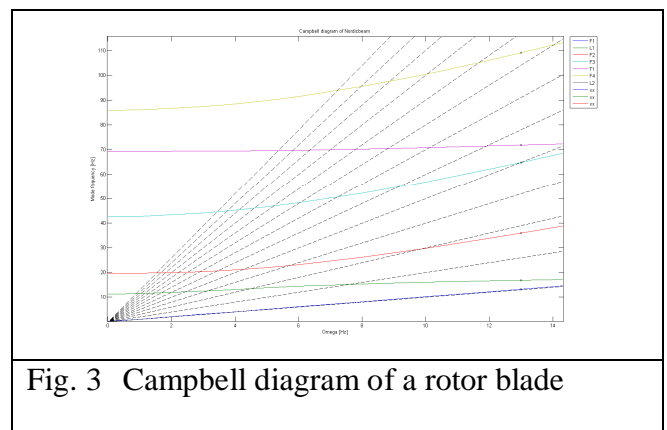


Fig. 3 Campbell diagram of a rotor blade

2.3 General structural non-linearities

Back lash and friction in various hinges have been investigated. Back lash is introduced by replacing a kinematic coupling with a non-linear spring. The stiffness of the spring element is adjusted so that there is a region with very low stiffness followed by a region with very high

stiffness. Being a work in progress, the inclusion of back lash is one item that is still under investigation.

Friction plays an important role in the model since centrifugal loads are relatively high. Friction is modelled using the built in friction models in Adams. Parameter studies on the influence of friction have been performed. Large rotations are handled by the MBD system, and material non-linearities are assumed negligible. Contact is currently handled using non-linear springs, but could be introduced more rigorously if needed.

2.4 The aerodynamic model

The aerodynamic forces and moments on the helicopter are driving the helicopter motion. It is hence essential to compute these accurately and efficiently. In order to reduce the simulation time, a simple but still accurate model has to be applied. This limits the model complexity. In the present study the lifting line approach has been adopted, see [1] and [2]. This means that the lift and drag forces and corresponding aerodynamic moments, on a rotor blade, are computed according to

$$F = \int \begin{bmatrix} D \cos \phi + L \sin \phi \\ 0 \\ L \cos \phi - D \sin \phi \end{bmatrix} dy \quad (1)$$

$$M = \int \begin{bmatrix} y(L \cos \phi - D \sin \phi) \\ -x_{cp}(D \cos \phi + L \sin \phi) \\ -y(D \cos \phi + L \sin \phi) \end{bmatrix} dy \quad (2)$$

where L is the lift and D the drag distribution, ϕ the induced angle of attack and x_{cp} the centre of pressure in the blade span direction. The local lift and drag are obtained from equation (3).

$$\begin{aligned} L &= \frac{1}{2} \rho U^2 c \cdot c_{l,\alpha} \cdot \left(\underbrace{\theta + \phi}_{\alpha} - \alpha_0 \right) \\ D &= \frac{1}{2} \rho U^2 c \cdot c_d \end{aligned} \quad (3)$$

Here ρ is the air density, U the local velocity of the air relative to the blade, c the blade chord and $c_{l,\alpha}$, c_d are aerodynamic coefficients. The force and moment contribution from the main and tail rotor are transferred to the helicopter body by standard coordinate transformations.

The induced angle is computed from the velocity U , the blade flapping velocity $\dot{\beta}$ and the down wash. The model for the down wash velocity includes the Glauert effect which is essential for obtaining a correct physical behavior of the helicopter in forward flight.

2.5 Coupling the aero and structural dynamic models

The aerodynamic model in section 2.4 has been implemented in the Adams frame work. The input to the aerodynamic model comes from the actual motions of the rotor blades (and helicopter frame). Deformation and motion of the blades contribute to the calculation of the angle of attack. Flap-wise, lag-wise and torsion-wise motions are all considered in the calculation of angle of attack. From the blade motion, aerodynamic forces are calculated and applied at different positions on the blade. The application point obviously rotates with the blade, but within the framework of the MBD-system, application of the force with time variant directions and positions is simply a matter of assigning the force to a moving coordinate system.

The discretisation of the external (aerodynamic) forces is done in 5 stations span-wise. This is a bit coarse, but has been proven to work well for many of the investigated cases so far. It is expected to be too coarse for high speed maneuvers, and will eventually be replaced by a finer discretisation or different numerical

integration. The helicopter normally operates with an advance ratio of $\mu < 0.2$ so the coarse discretisation is of only limited concern. The calculation of aerodynamic forces can be done for test cases outside of the MBD package, where comparisons of different discretisations can easily be done. Due to the chosen implementation of the aerodynamic force inclusion, it is not feasible to add points of action at will. Use of user sub-routines in the MBD package would make adding points easier and is planned for future evolutions of the model.

Drag force on the helicopter frame is also included using a square plate analogy.

2.6 Control system/autopilot

The helicopter is by nature an unstable configuration, and as such, a control system for setting up and maintaining a flight conditions is needed. The numerical model includes an enhanced PID-regulation to perform this. The PID regulation includes position error feedback (P), time integrated position error (I) and time derivative position feedback (velocity) (D). Since the motion is also dependant of the attitude of the rotorcraft, the control loop is also fed by attitude (A) and attitude rates (W). The PIDAW schematic is pictured in Fig. 4. In the control system, this part is used in a closed loop.

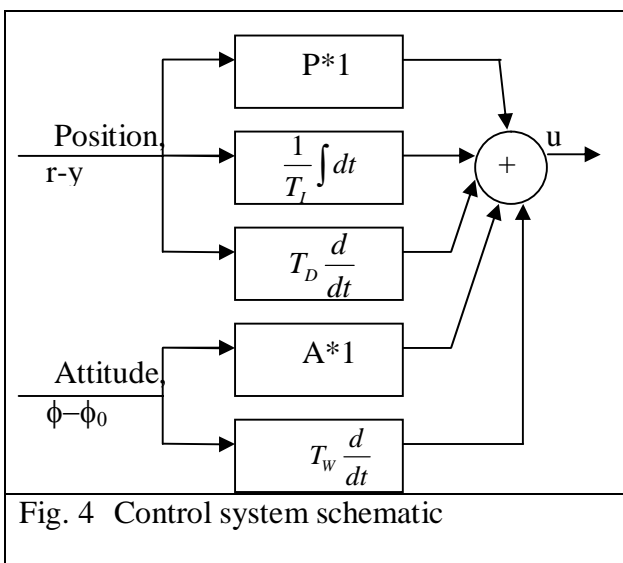


Fig. 4 Control system schematic

Independent control loops exist for pitch and roll respectively. For controlling yaw and collective (average lift), a simpler PID regulation is adequate. Yaw and collective is controlled by independent control systems adding a total of four independent control systems for handling the rotorcraft.

For some rotor system configurations, the inherently strong cross couplings between roll and pitch responses to roll and pitch commands make the adjustment of good (independent, indirectly coupled) control systems difficult. Trimming of the gains P,I,D,A and W have been done in an iterative manner to get an autopilot that is good enough for current simulation purposes. There are probably better ways to set up such systems, but it was not the main objective for the model. It is noted that the regulation gains need to be adjusted if major changes are done in the dynamical system, see below.

All measures for the control system are taken at the centre of gravity (CG) of the helicopter. A low pass filter is applied to the angle rate signals to make regulation smoother.

An example of the control system performance is given in Fig. 5, where normalized pitch and roll rates are plotted for a startup sequence. With blades initially at rest, the rotor system is quickly spun up to nominal speed and command to hover at a specific point in space is given. With no available force at the blades (they are spinning too slowly in the first seconds), very large control signals is requested by the autopilot. However, despite this very large disturbance, the rotorcraft comes to rest at hover quite quickly.

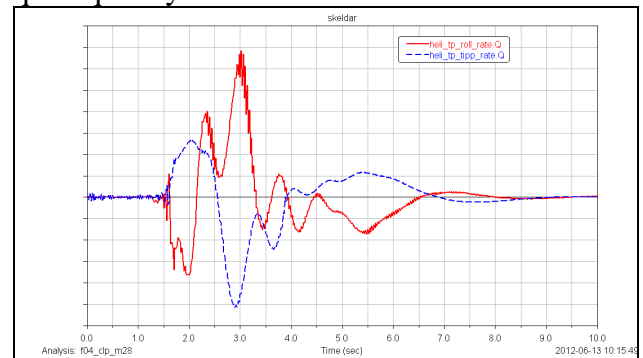


Fig. 5 Attitude rates for a startup sequence

3. The assembled model

The system is driven by applying a rotation or torque to the main shaft relative to the helicopter frame. This will cause the rotor to spin counter clockwise, but will also cause a counter reaction that will turn the whole helicopter clockwise. A simplified tail rotor force is therefore also applied, with its own PID-control to keep the rotorcraft heading steady. Using a force instead of simply applying a rotation constraint gives a better representation of the physics with e.g. a slight roll attitude of the rotorcraft needed at hover. In addition to the applied main torque, control servos are controlled by the autopilot. The motion of the rotor blades will result in applied external aerodynamic loads. The loads will cause the helicopter to move, and this motion is picked up by the autopilot which in turn controls the rotation of the servos. There are no other external forces or motions applied, and if modelled correctly, the motion of the rotorcraft is given by the modeling of the external aerodynamic loads only. No fictitious assumptions about motions or inclusions or reductions of physical laws are done. Being a simulation model it is easy to measure everything in the rotor system. It can also be beneficial to apply a camera at the rotor hub pointing outward to view the dynamic motion of one blade. This is something that is not so easy (but possible) to do in real life. The understanding of the dynamics in the rotor system is greatly enhanced by the opportunity to animate any part of the system or extract motions or forces as curves at will.

4. Results and comparisons

To gain confidence in the model, several tests and measurements have been performed. Section 4.1 gives a verification of the model and comparisons to tests. In Section 4.2 the rotor design is discussed.

4.1 Model analysis

This section describes verification and analysis of the model.

4.1.1 Modal analysis of the rotor blades

Rotor blades are the core of the rotor system, and have to be represented in a good fashion. Comparisons of the modelled blades have been done with static modal measurements. After smaller adjustments, the table below shows a comparison:

Mode	Measured frequency [Ω]	Calculated frequency [Ω]	Difference [%]
F1	0,32	0,31	-1.7
L1	1,45	1,45	-0.5
F2	1,95	2,02	3.5
F3+T	5,48	5,79	5.8
T1	5,64	5,85	3.7
F4	11,31	11,52	1.8

Table 1. Blade mode comparison

4.2 Rotor rig tests

When the blades are well modelled, the complete rotor system should also be tested. Since this is a rotating system, measuring in rotating parts is not trivial. Measurements of blade moments and flap motion have been performed and compared to the model. A flap motion measure comparison is given in Fig. 6 below.

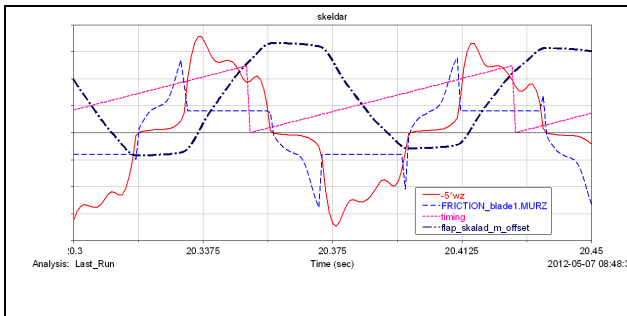


Fig. 6 Simulated flapping

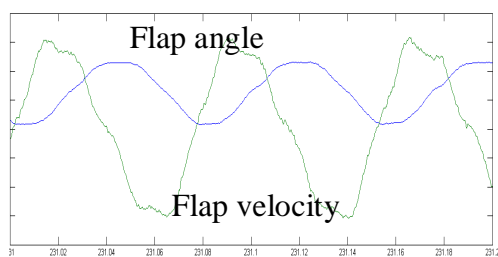


Fig. 6b Measured flapping

The first diagram gives results from a simulation including static and dynamic friction in the flap hinge. Normalised flap angle is represented by a black dot-dashed line. Flap velocity is shown in a red colour. The second diagram in Fig. 6 shows normalised measured data from a rotor-rig. The overall shape of the flapping motion is well captured in the model. In the first diagram, the calculated resulting friction coefficient is also pictured as a blue dashed curve. For a well functioning flapping hinge, the flapping motion should be close to a sinusoidal shape.

4.2.1 Flight tests

Finally, the response of the rotorcraft given a specified control input should also be validated. An example of this is given in Fig. 7, where actual flight control input for a test case was also fed to the simulation model. The modelled system and the real life system are not completely equal, e.g. wind was not measured during flight. However, the pitch and roll rate response of the modelled rotorcraft was reasonably good even for this test. In the figure, measured roll and pitch rates use solid blue and

green lines, while simulated data is represented by dashed lines.

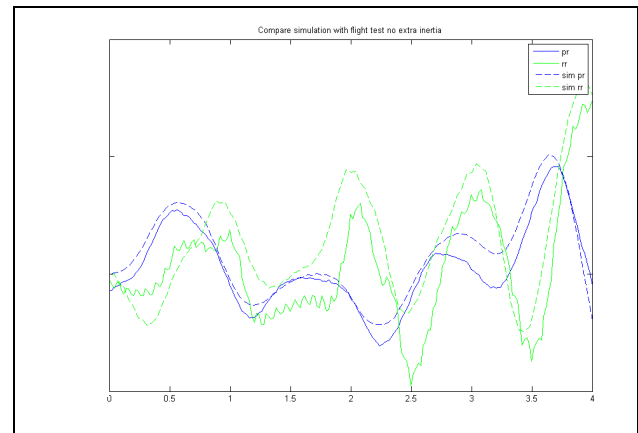


Fig. 7 Comparison of simulated flight with measured data

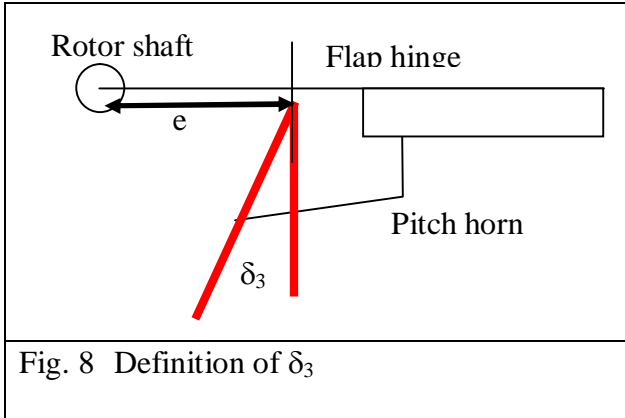
For more controlled tests in no wind using smaller input, the response in the model compares even better to measured data.

4.3 Rotor system design

With a model that gives good enough correlation to flight tests it makes sense to use it for design evaluations. In the simulation model it is easy to introduce changes and evaluate how rotorcraft performances change. Understanding the root cause for e.g. cross couplings in a given system is essential to reduce the problems associated with it. Also evaluating performance for complete system changes (e.g. changing to a teetering rotor system) is both easy and necessary before spending time and money on major changes. A few investigated design changes are discussed below.

4.3.1 The effect of flap-pitch coupling, δ_3

The δ_3 angle in rotorcraft is usually defined as the angle between the application point of the pitch horn to the flap hinge axis, see Fig. 8.



If this angle is positive, like in the figure, the pitch of the blade decreases with increasing flapping of the blade. This in turn causes the resonant rotor disc system to change frequency and is perceived as a damping of the flapping motion. With a functioning flap hinge, the normalised flapping frequency can be expressed as

$$\lambda = \sqrt{1 + \frac{3e}{2} + \frac{\gamma}{8} \tan(\delta_3)} \quad (14)$$

Where e is the hinge offset defined in Fig. 8 and γ is the Lock's number. Normalisation is done using rotor radius and rotor speed, respectively. A positive δ_3 increases the virtual stiffness and flap frequency, while a negative δ_3 reduces the flap frequency.

δ_3 is usually applied to reduce sensitivity to external disturbances like wind, but also causes control authority to decrease. A δ_3 angle of 45 degrees completely eliminates cyclic control of the disc. Collective control is still possible however, and this is used in various tail rotor configurations to improve performance and reduce wind/speed sensitivity of the tail rotor. Changes to δ_3 were investigated to see how it influences cross couplings relative to the reference rotor system.

The effect of using a negative δ_3 is actually similar to using a positive δ_3 , but instead of increasing the disc frequency, it reduces the disc frequency. The perceived damping is still about the same. It can be shown that negative δ_3 is stable for hover conditions, and investigations

on stability for forward speed conditions is currently under investigation, see [3] and [4]. The effect of applying a negative δ_3 in the reference rotor system is given in Fig. 9.

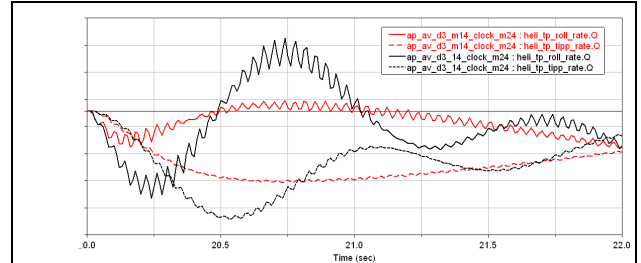


Fig. 9 Influence of negative δ_3 on pitch and roll rates in a reference rotor system

Normalised attitude rates are given as a function of time. From the figure it is noted that applying a negative δ_3 actually reduces the inherent cross coupling between pitch and roll motion for a pitch step input.

4.3.2 Influence of teetering hinge

A way of balancing the centrifugal loads is to introduce a teetering hinge. By allowing the centrifugal loads of the two blades to counteract each other only a small portion of the bearing load remains that can cause friction. Thus, the resulting friction torque will decrease.

Model wise, this is very easy to introduce, and the effects in performance can also easily be investigated. By introducing a third hinge at the top of the main shaft, see Fig. 10 below, a teetering rotor system can be analysed.

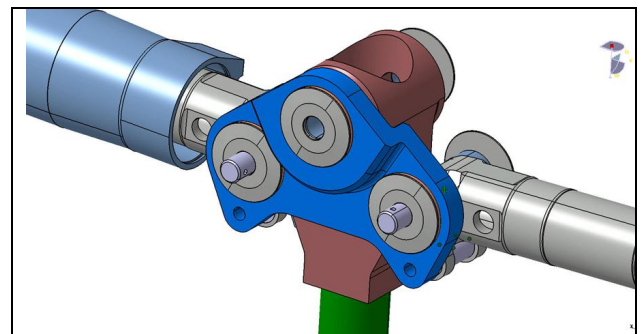


Fig. 10 Overview of a teetering hinge design

Fig. 11 shows a comparison of normalised pitch and roll rates for teetering and reference rotor systems.

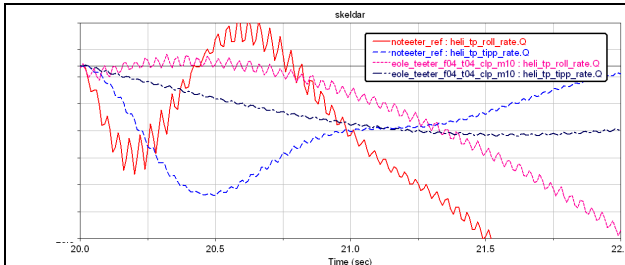


Fig. 11 Influence of introducing a teetering hinge on pitch and roll rates in a reference rotor system

Note that the cross coupling is greatly reduced for the teetering system, but also that the response time is a lot longer. This is common knowledge in rotor industry and is captured well in the model.

5. Conclusions

A coupled aerodynamics and structural dynamics model has been developed and implemented in the software MSC/Adams. The numerical model has successfully been used to capture the behavior of existing rotor systems. Correlation to rig tests and flight test data shows good model characteristics. Using modeling of physics to introduce all external and internal loads in addition to a user friendly representation and use of geometrical and kinematical data and constraints, the simulation model can be very useful in rotor system development. By introducing various design changes to the correlated simulation model, expected system behaviour can be analysed before actual flight tests.

The model has been useful in understanding the characteristics in the current rotor system in Skeldar V200.

6. References

- [1] Leischman *Principles of Helicopter Aerodynamics*. 2nd edition, Cambridge University Press, 2006.
- [2] Bramwell A. R. S, Done G. and Balmford D. *Helicopter Dynamics* 2nd edition, Butterworth-Heinemann, 2001.
- [3] Figueira J.M.P., Cruz R and Andrade D., The influence of the positive pitch-flap coupling (negative δ_3) on the flapping response of an articulated tail rotor. 9th Brazilian Conference on Dynamics, Control and their Applications, DINCON'10, June 2010.
- [4] Gaffey T.M., Pitch-flap Coupling (Negative δ_3) on Rotor Blade Motion Stability and Flapping, JAHS, April 1969.

7. Copyright Statement

The authors confirm that they, and/or their company or organization, hold copyright on all of the original material included in this paper. The authors also confirm that they have obtained permission, from the copyright holder of any third party material included in this paper, to publish it as part of their paper. The authors confirm that they give permission, or have obtained permission from the copyright holder of this paper, for the publication and distribution of this paper as part of the ICAS2012 proceedings or as individual off-prints from the proceedings.